Development of a P300 Brain-Machine Interface and Design of an Elastic Mechanism for Rehabilitation Robot

Han-Pang Huang, Yi-Hung Liu, Wei-Zhi Lin, Zhi-Hao Kang, Ching-An Cheng, and Tzu-Hao Huang

***Abstract*—This paper focus on the development of P300 speller and design of a rehabilitation robot for brain machine interface. This research method mainly points out a norm which can be used to recognize whether the individual's independence is increasing or decreasing comparing with the original signals after extracting and composing some different features. The result shows that this feature combination, SMCF, can keep 90% sorting rate when the "Round" number is 5, also it can reduce the relationship of individual independence. Among the results, the highest value can increase to 36.04%.**

On the other hand, considering the interaction between people and machines under safety constraints without utilizing difficult and complex control strategies, this paper proposes a new actuator design, adaptive coupled elastic actuator (ACEA) with adjustable characteristics adaptive to the applied output force and input force. This would provide oncoming robotic systems with an intrinsic compromise between performance and safety in unstructured environments; namely, exhibiting desired intrinsic lower and higher output impedance depending on different operation situations. Finally, experimental results are presented to show the desired properties of the proposed ACEA system.

I. Introduction

Brain-computer interface (BCI) is a communication channel that does not require peripheral nerves or muscles; hence it provides a user with a direct communication channel which sends commands to electronic devices by means of brain activities[1], which is very helpful for people with serve motor disabilities. Electroencephalogram (EEG) signal, due to its high temporal resolution, has been the most frequently used input to BCI systems. The P300 potential is a response to an infrequent stimulus. It usually appears in EEG signals around 300ms after the infrequent stimulus occurs. The most typical BCI system which uses P300 potentials as an input would be the P300 speller proposed by Farwell and Donchin [2][3], in which the P300 visual evoked potential is elicited by an oddball paradigm. The P300 speller BCI system is able to detect which character in the spelling matrix is the target that the user is focusing on, and then show the detection result (target character) on the screen, thereby enabling lock-in people communicate with others. Previous works related to P300 speller BCI's have utilized various two-class classifiers to solve this problem. Hoffmann et al[4]. used the boosting with orthogonal least square (OLS) as the classifier. Lenhardt et al. [5] and Bostanov [6] utilized the linear discriminant analysis (LDA) method to maximize the separation between classes. Based on the LDA, a Bayesian LDA (BLDA) classifier was further proposed in [7] and has been used in a P300 speller paradigm [8]. The support vector machine (SVM) has also shown satisfactory results in P300 BCI systems [9]. More recently, the SVM ensemble has shown to be better than one single SVM in solving the problem of P300 detection [10]. The success of SVM in those P300 BCI's should be attributed to the facts that it plays kernel tricks and its formulation embodies the principle of structural risk minimization [11], providing better generalization ability than the traditional learning machines such as the neural networks trained by error back-propagation algorithm [12].

About the development of robots as mechanical workers that can support human labor and assist human daily activities by physical interaction, informational interaction, etc., has been expected for a long time. That is why, recently, the field of physical human-robot interaction (pHRI), considering the trade-off between safety and performance, emerges from modern robotics as a focused effort to design manipulators intrinsically safe for human interaction [13].

Traditionally, modifying the controllers of rigid robots by additional sensors has demonstrated the effectiveness of achieving safe manipulation [14]. However, the intrinsic properties of a controller restrict the dynamic performance of a robot because of the unmatched mechanical bandwidth. Furthermore, the natural dynamics of the system may be affected by extrinsic dynamic behavior due to the energy loss caused by the software control system.

Specifically, the most critical feature of modern actuator designs is the stiffness constant of the series elastic component, a physical quantity which dominates the bandwidth and payload capacity of the overall system and the safety level of the pHRI. It is also worthwhile to mention that designing this kind of system should always determine a maximum allowable output impedance and a maximum tolerable striction on the system to define the upper bound of the stiffness constant, and a minimum acceptable large force bandwidth to define the lower bound of the stiffness constant [15]. In addition, among those systems, stiff ones exhibit more rapid responses to load change and more capacity to handle heavy objects, whereas with respect to the pHRI, they may result in a more acute impulse shock to harm humans seriously. On the contrary, soft ones exhibit slower responses to load change and less capacity to handle heavy objects,

H. P. Huang is with the Department of Mechanical Engineering, National Taiwan University, Taipei, Taiwan, 10617, R.O.C. (Corresponding addressee e-mail: hanpang@ntu.edu.tw).

Y. H. Liu is with the Department of Mechanical Engineering, Chung Yuan Christian University, Chung-Li 32023, Taiwan, R.O.C. (e-mail: lyh@cycu.edu.tw).

W. Z. Lin, Z. H. Kang, C. A. Cheng, and T. H. Huang are with the Department of Mechanical Engineering, National Taiwan University, Taipei, Taiwan, 10617, R.O.C.

whereas focusing on the pHRI, they do have intrinsic safety motions to protect humans during manipulation. In general, a compromise between safety and performance is difficult to achieve.

The major objective is to provide an inherently adjustable series elastic device for physical human-robot interaction. Herein, a new actuator, namely an adaptive coupled elastic actuator (ACEA) with adjustable characteristics adaptive to the applied output force and input force is developed.

II. Materials and Methods

A. Data Acquisition and Preprocessing

Our system uses six monochannels. Each channel receives EEG signals from a distinct electrode. The six electrodes are placed on Fz, Fcz, Cz, Pz, P7, and P8 in the 10-20 system, respectively. The potential measured from each of the first four (Fz, Fcz, Cz, pz) is further subtracted by the average of P7 and P8 potentials. At the preprocessing stage, a 0.1-70 Hz band-pass filtering is performed. The acquired EEG signals are amplified with the gain of 24,000. The signals are then converted to digital ones and sent into a computer via the DAQ-6212 produced by National Instrument. The received digitized EEG signals are called EEG data.

At the computer side, the data collection task is done by our own software written in C#. The EEG data are collected at a sampling rate of 250 Hz. The software has three parts. The first part presents the 6 x 6 spelling matrix (Fig. 1) and the intensification (stimulus) of the row or column. The second part is responsible for sending the corresponding stimulus code to be embedded in the data stream in a time-locked manner when a stimulus is presented. By the stimulus code, the first 500-ms data (an epoch) from each channel can be automatically obtained.

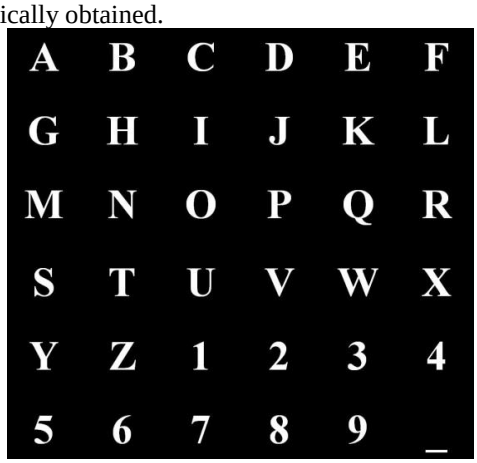

Fig. 1. P300 speller.

B. Training Data Collection

Our data collection procedure, mainly following the one suggested in [16], contains three stages: 1) preparation; 2) training set collection; 3) test set collection stages.

Fig. 2. Data collection for a subject. The computer is placed behind the blue shield.

During the preparation stage, an electro-cap is attached to a subject. An electrolyte gel is applied to the electrodes to reduce the impedance. The subject sits at the position around 90 cm in front of a 17-inch liquid crystal display (LCD) (see Fig. 2.). During the training stage, the subject is asked to focus on a sequence of characters given by the experimenter, one character at a time. First, one of the characters is intensified on the LCD for 4 s, by which the subject can direct his\her focus to the position of this character. After the attention-catching intensification, a 2.5 s preparation gap is given before a data collection procedure. During this procedure, the subject is asked to focus on the target character, and then the system will initiate a 10-round intensification process, where within each round, 12 randomly-ordered visual stimuli will be presented. Each stimulus is the intensification of either one row or one column, and will be presented for 100 ms, and after a 75 ms inter-stimuli interval, the next stimulus will be presented. After presentation of 10 stimuli, a round is ended, and after a pause of 0.5 s, the next round begins. Therefore, a 10-round intensification process will take 27.75 s.

At the computer side, the data collection task is done by our own software written in C#. The EEG data are collected at a sampling rate of 250 Hz. The software has three parts. The first part presents the 6 x 6 spelling matrix (Fig. 2) and the intensification (stimulus) of the row or column. The second part is responsible for sending the corresponding stimulus code to be embedded in the data stream in a time-locked manner when a stimulus is presented. By the stimulus code, the first 500-ms data (an epoch) from each channel can be automatically obtained. Namely, when a particular row or column is intensified (flashed), we get the vector

$$\mathbf{x} = [x_1(1), ..., x_1(N), x_2(1), ..., x_2(N), x_K(1), ..., x_K(N)]^T \quad (1)$$

where K and N denote the number of channels and the number of samples, respectively, and xi(j) denotes the jth sample from the ith channel. Here, N = 125 and K = 4.

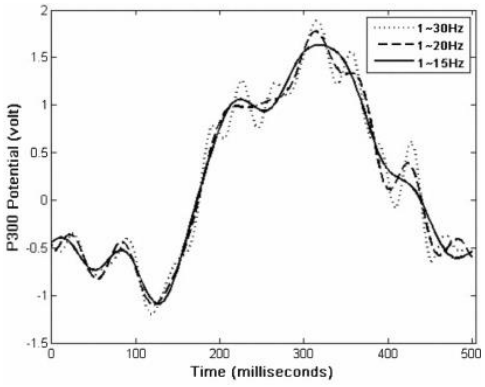

Fig. 3. Band-pass filtered P300 potentials using inverse DFT. The X axis is the time from the stimulus presentation.

Fig. 3.Fig. 3 shows P300 potentials recorded from Pz. Moreover, it is also found that the SVM achieve the best classification accuracy when the frequency band is set as 1 -15 Hz. With this band, the SNR of the EEG signals can be greatly increased, since the 60-Hz line noise is completely removed and the impact from electromyography (EMG) signals (10 -400 Hz [17]) is substantially reduced. However, such reconstruction is unable to remove electrooculography (EOG) signals since EOG signals lies in low frequencies smaller than 10 Hz [18]. To avoid the ocular artifacts, the subjects were asked not to make any eye movements during the experiments.

C. Feature extraction and Classification

Feature extraction can be divided into two parts : 1) the EEG signal superposition of the average after feature extraction, there are three features of the area, N100 and P300 time and slope. 2) the EEG signal is depicted in a binary image, and turn it into a closed curve by using the boundary extraction algorithm (BEA) [19]. The edge of the binary image recorded by Fourier descriptors. Then the edge information into the form of frequency data and we can obtain the edge of the center (x_{center},y_{center}).

(a) Area
Sum of the EEG signal between 200ms to 500ms.
(b) Time of N100 and P300
N100(trough) and P300(peak) time.
N100:50ms~170ms
P300:220ms~500ms
(c) Slope

$$m = \frac{P300\_volt - N100\_volt}{P300\_time - N100\_time} \quad (2)$$

P300_volt : *P300* peak value.
N100_volt : *N100* trough value.
P300_time : P300's time.
N100_time : N100's time.
(d) Fourier Descriptor (FD) [20] and Center
Assume that the edges of an image can make use of the Cartesian coordinate system, so we can get the following coordinates on ($x[m]$,$y[m]$),m=1,2,…,L (L: The total number of the edges of the image). By these coordinates on ($x[m]$,$y[m]$), equation ($a[n] = \frac{1}{L}\sum_{m=1}^{L} x[m]e^{-jnw_0 m}$ (3) and ($b[n] = \frac{1}{L}\sum_{m=1}^{L} y[m]e^{-jnw_0 m}$ (4) can get the Fourier coefficient ($a[n]$,$b[n]$).

$$a[n] = \frac{1}{L}\sum_{m=1}^{L} x[m]e^{-jnw_0 m} \quad (3)$$

$$b[n] = \frac{1}{L}\sum_{m=1}^{L} y[m]e^{-jnw_0 m} \quad (4)$$

$$s[n] = \frac{r[n]}{r[1]}, \quad r[n] = \sqrt{|a[n]|^2 + |b[n]|^2} \quad (5)$$

By equation ($s[n] = \frac{r[n]}{r[1]}$, $r[n] = \sqrt{|a[n]|^2 + |b[n]|^2}$ (5) we can get the Fourier descriptor $s[n]$.

$$x_{center} = \frac{\sum_{m=1}^{L} x[m]}{L} \qquad y_{center} = \frac{\sum_{m=1}^{L} y[m]}{L} \quad (6)$$

Using equation ($x_{center} = \frac{\sum_{m=1}^{L} x[m]}{L}$ $y_{center} = \frac{\sum_{m=1}^{L} y[m]}{L}$ (6) can get the center of the edge (x_{center},y_{center}).

We use the support vector machine as classifier after feature extraction. In SVM, the training set is given as $\{x_i, y_i\}_{i=1}^{n}$ where $\mathbf{x}_i \in R^d$ are the training patterns and $y_i \in \{-1, +1\}$ are the class labels. Here, d = 500. Let w and b be the weight vector and the bias of the separating hyperplane, respectively, the objective of SVM is to find the optimal hyperplane by maximizing the margin of separation and minimizing the training errors, formulated as the optimization problem:

$$\begin{aligned} &\min_{f,b,\xi} \frac{1}{2}\|w\|^2 + C\sum_{i}^{N}\xi_i, && \text{for } i = 1, 2, ..., N, \\ &s.t.\ \ y_i(w^T\phi(x_i) + b) \geq 1 - \xi_i, && \forall i, \\ &\xi_i \geq 0, && \forall i. \end{aligned} \quad (7)$$

The dual problem of SVM is as follows:

$$\max_{f,b,\xi} \quad -\frac{1}{2}\sum_{i,j}^{N}\alpha_i\alpha_j y_i y_j K(x_i,x_j)+\sum_{i}^{N}\alpha_i, \quad \text{for } i=1,\ 2,\ .....,\ N,$$

$$\text{s.t.} \quad \sum_{i}^{N}\alpha_i y_i, \tag{8}$$

$$0\le\xi_i\le C, \qquad \forall i.$$

Finally, we can obtain the decision function:

$$f(x)=\sum_{i}^{N}\alpha_i^* K(x,x_i)+b^* \tag{9}$$

The kernel type is chosen as Gaussian kernel:

$$K_{Gaussian}(x_i,x_j)=\phi(x_i)\phi(x_j)^T=\exp(-\frac{\left\|x_i-x_j\right\|_2^2}{2\sigma^2}) \tag{10}$$

The cross-validation is chosen as 2-fold and 10 runs. SVM determines the most probable row and column by the following two decision functions:

$$r^*=\arg\max_{r=1,\ldots,n_r}\{\sum_{i=1}^{n}\alpha_i y_i k(x_{row}^{(r)},x_i)+b\} \tag{11}$$

$$c^*=\arg\max_{c=1,\ldots,n_c}\{\sum_{i=1}^{n}\alpha_i y_i k(x_{col}^{(c)},x_i)+b\} \tag{12}$$

where n_r and n_c are the number of row and the number of column in the character matrix, respectively($n_r = n_c = 6$), and α_i are Lagrange multipliers. Once the indices are determined, the character is recognized.

III. Rehabilitation System

A. Design Concept of ACEA

Utilizing a set of two different elastic components, one with soft stiffness and the other with hard stiffness, may alleviate the aforementioned drawbacks of traditional SEA systems. A new approach adaptive coupled elastic actuator (ACEA) is proposed, and the model is shown in Fig. 4, where M_l, X_l and F_l denote the link mass, displacement of the output link and force on the link; M_m, X_m and F_m denote the actuator mass, displacement of the actuator and input force of the actuator; K_s and K_h denote stiffness of the soft and hard elastic elements, respectively.

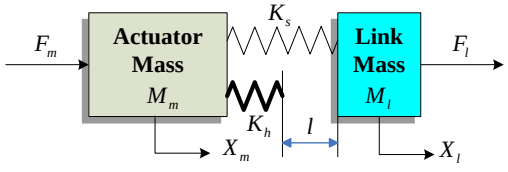

Fig. 4. Model of proposed adaptive coupled elastic actuator.

Herein, by assuming that the total compression distance $\Delta X_s=(X_m-X_l)$ is always positive or equal to zero and defining that the critical length $l(t,\Delta X_s)$ is the difference in displacement between the positions of the hard elastic element and the output link at time t, the equivalent transmission stiffness of the ACEA approach can be shown as

$$K_t=\begin{cases}K_s, & \text{if } F_l\le F_{th} \text{ or } l(t,\Delta X_s)>0\\ K_h+K_s, & \text{otherwise}\end{cases} \tag{13}$$

where $F_{th}=K_s\cdot l(t,0)$ is the threshold force that equals to K_s multiplying the preset critical length $l(t,0)$ associated with $\Delta X_s=0$, and $F_l=K_s\cdot\Delta X_s$ is the restored force provided by the deflection when the soft elastic element is stressed. The critical length l that should be adaptive to the applied output force and input force decides the inherent stiffness of the actuation approach, meaning that the system is capable of dividing the total input force into direct driving and stiffness shifting forces, two forces which both contribute to the output force. Thus, the ACEA can be thought to divide the torque generation into separate low- and high-frequency parallel actuators by adjusting l adaptively, as shown in Fig. 5.

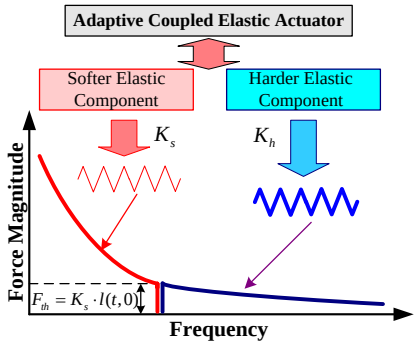

Fig. 5. Concept of adaptive coupled elastic actuator: partition of torque into low and high frequency components.

By varying an adjustable l accompanied by proper active control, the actuator may obtain any desired threshold force/torque adaptive to task-oriented strategies. Compared to the previous compliant or stiff actuators, such as SEA, the actuators utilizing the proposed ACEA approach exhibit the desired intrinsic lower or higher output impedance. The relationship between an external load and deflection can be seen in Fig. 6, and the roughly proposed operation states of an ACEA system can be seen in Table 1.

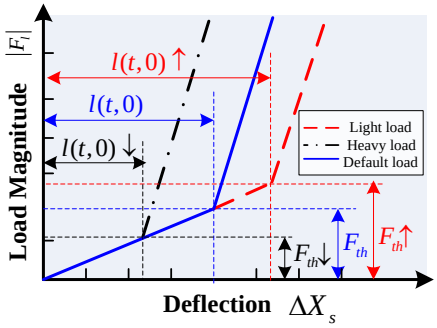

Fig. 6. Properties of adaptive coupled elastic actuator: the relationship between load and deflection.

Table 1 Different proposed operation state of an ACEA system

Operation speed	Hard elastic element	Soft elastic element
High	Performance	Interaction
Low	Performance and Interaction	Interaction

B. Mechanism Design

In brief, the critical issues of the ACEA system are how to design a mechanism and a control system to adjust and determine the stiffness of the soft and hard elastic components in advance. As shown in Fig. 7, the ACEA actuator, utilizing only one actuator, is designed to provide a favorable solution to adjust the critical length by a torque switch mechanism.

In this design, a worm drives a worm gear through two sets of preloaded soft linear compression springs, initially restraining the movement of the worm shaft in its axial direction. One set of hard linear compression springs will restrain the movement of the worm shaft in its axial direction while the critical length becomes zero.

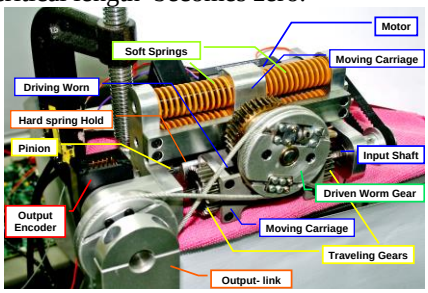

Fig. 7. One-DOF adaptive coupled elastic actuator.

Specifically, the torque switch mechanism consists of a pair of traveling gears and corresponding pinions to drive a both-end-thread screw that can simultaneously convey two movable hard spring holders along the screw. This mechanism can channel and switch the input torque into either direct output torque or input torque to adjust the critical length, permitting the ACEA to vary according to the load torque and the input torque. Via the torque switch mechanism, the system can mechanically alter the critical length/force in response to a light load within the first range of handling a relatively light load or within the first range of quickly operating to make small output impedance responses, or in response to a heavy load within the second range of handling a relatively heavy load or the second range of slowly operating to make large output impedance responses.

IV. Experiment Results

A. P300 experiment results

First, we discuss the relationship between the numbers of Fourier descriptors to its accuracy. As you can see from Fig.8, select more than four Fourier descriptors as the feature has maintained the same accuracy, but the number of features will increase the computational complexity. Therefore, we only took the first four Fourier descriptors as a feature, said FD4.

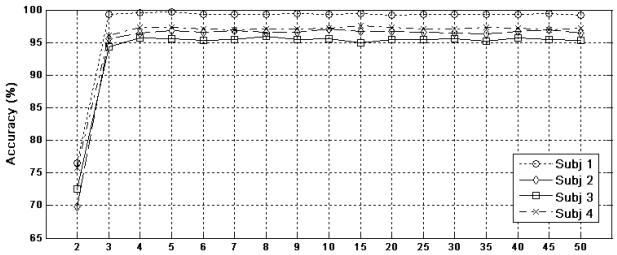

Fig. 8. The relationship between different Fourier descriptors and classification rate.

On the experimental results, take the beginning of the letters to represent features. i.e. A as area, S as slope,…,etc. Raw represents the original data. Rounds rear brackets show the training time.

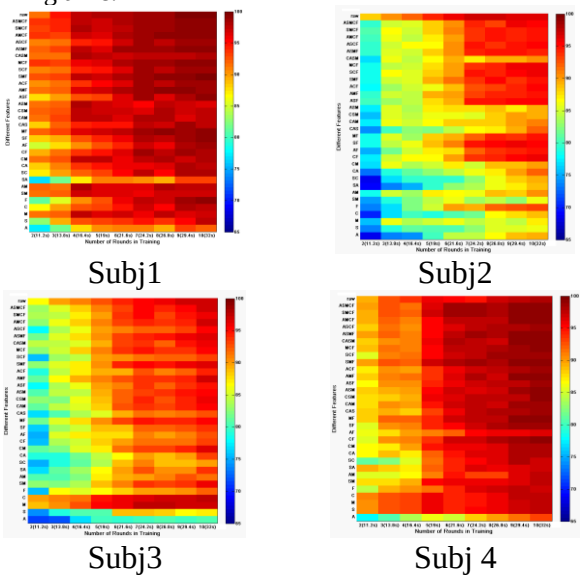

Fig. 9 The different feature extraction combination of classification results

In Fig. 9, if only consider the A, S, M, C and F the five individual features. The A feature is the worst result. M and F have the better results. More combinations of features, its accuracy has increase the trend in addition to Subj2. The combination of ASMCF can be maintained the similar accuracy with the raw data. We see SMCF feature combination will be able to maintain the classification rate as raw data. In addition, you can find a combination containing F features, its accuracy had good results by Subj2 can clearly see that the feature of F containing a combination of accuracy has significantly improved. The different combination of features will have different results, and will have different effects in different subjects, such as M and C of these two features, in Subj2 and Subj3 can get two different results. Therefore we chose the combination of features enhance the effect for Subj1 to Subj4 have to continue to explore the relationship for individual independence.

Table 2 Raw data of individual independence test
the results of the accuracy (%)

Subj	1	2	3	4
1	98.78	64.02	62.80	68.90

2	62.32	95.12	71.95	82.32
3	72.07	81.10	98.78	75.73
4	75.12	65.37	67.80	96.34

Table 3 SMCF features of individual independence test
the results of the accuracy (%)

Subj	1	2	3	4
1	98.78(0)	84.76(32.38)	84.15(33.98)	93.73(36.04)
2	75.73(21.53)	92.46(-2.79)	82.93(15.25)	90.02(9.36)
3	75.12(4.23)	84.76(4.51)	91.46(-7.41)	75.73(0)
4	75.64(0.69)	61.71(-5.6)	78.41(15.65)	98.78(2.53)

B. Human-Robot Interaction

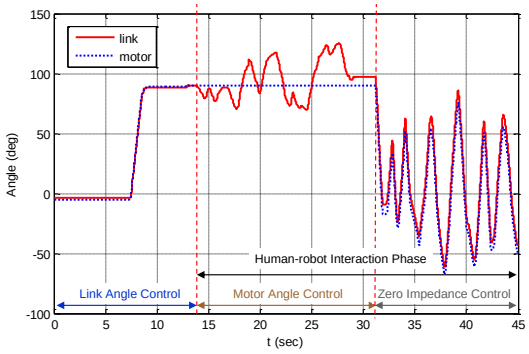

Fig. 10. Human-robot interaction experiment under three control modes.

The dynamics of a robotic system can be drastically changed by interaction with a human operator, since the motion of the human is too complicated to be modeled or predicted.

Herein, the control mode of the designed system was chosen to match different operating situations according to whether the robot was interacting with a human operator. In the beginning, the robot was set to track the given output link trajectory without any interaction between human, robot, or environment under the output link angle control. Then, the human operator tried to randomly guide the output link under the motor angle control or zero impedance control.

The experimental results, shown in Fig. 10, demonstrated that the robot can track the given output link trajectory quite well under output link angle control in spite of the effect of the link dynamics as the main resistive torque source. Because of the flexibility of the joint, the human operator can force the robot to move as the operator wanted, whereas the robot only allowed the operator to partially backdrive the output link under the motor angle control. However, the operator could randomly guide the robot easily under zero impedance control, where the desired output torque is regulated to be zero, even if some relatively small resistive torque was observed in the experiment.

V. CONCLUSION

The P300 result shows that this feature combination, SMCF, can keep 90% sorting rate when the “Round” number is 5, also it can reduce the relationship of individual independence. Among the results, the highest value can increase to 36.04%. About the rehabilitation robot, the design, model, and control of a new ACEA actuator for human-robot interaction is developed. Possessing adjustable characteristics through a novel Torque Switch mechanism, it is proposed to handle different loads or to make different output impedance responses while guaranteeing safety issues.

Finally, this P300 Speller and ACEA design already provide upcoming robots with intrinsic safety in compromise with performance in complex environments in our ongoing work.

ACKNOWLEDGMENT

This work is partially supported by the National Science Council of the R.O.C. under grants NSC 100-2221-E-002-12 7-MY3 and NSC 100-2221-E-002-077-MY3.

REFERENCES

[1] N. B. J. R. Wolpaw, D. J. McFarland, G. Pfurtscheller, and T. M. Vaughan, "Braincomputer interfaces for communication and control," *Clinical Neurophysiology*, vol. 113, No. 5, pp. 767-791, 2002.

[2] L. A. Farwell and E. Donchin, "Talking off the top of your head: Toward a mental prosthesis utilizing event-related brain potentials," *Electroencephalogr. Clin. Neurophysiol*, vol. 70, No. 6, pp. 510-523, Dec. 1988.

[3] E. Donchin, K. M. Spencer, and R. Wijesinghe, "The mental prosthesis: assessing the speed of a P300-based brain-computer interface," *IEEE Transactions on Rehabilitation Engineering*, vol. 8, No. 2, pp. 174-179, 2000.

[4] U. Hoffmann, G. Garcia, J. Vesin, K. Diserens, and T. Ebrahimi, "A Boosting Approach to P300 Detection with Application to Brain-Computer Interfaces," *International IEEE EMBS Conference on Neural Engineering*, Washington D.C., USA, 2005, pp. 97-100.

[5] A. Lenhardt, M. Kaper, and H. J. Ritter, "An Adaptive P300-Based Online Brain-Computer Interface," *IEEE Transactions on Neural Systems and Rehabilitation Engineering*, vol. 16, No. 2, pp. 121-130, 2008.

[6] V. Bostanov, "BCI competition 2003-data sets Ib and IIb: feature extraction from event-related brain potentials with the continuous wavelet transform and the t-value scalogram," *IEEE Transactions on Biomedical Engineering*, vol. 51, No. 6, pp. 1057-1061, 2004.

[7] U. Hoffmann, J. M. Vesin, T. Ebrahimi, and K. Diserens, "An efficient p300-based brain-computer interface for disabled subjects," *J. Neuroscience Method*, vol. 167, No. 1, pp. 115-125, 2008.

[8] B. Rivet, A. Souloumiac, V. Attina, and G. Gibert, "xDAWN Algorithm to Enhance Evoked Potentials: Application to Brain Computer Interface," *IEEE Transactions on Biomedical Engineering*, vol. 56, No. 8, pp. 2035-2043, 2009.

[9] M. Kaper, P. Meinicke, U. Grossekathoefer, T. Lingner, and H. Ritter, "BCI competition 2003-data set IIb: support vector machines for the P300 speller paradigm," *IEEE Transactions on Biomedical Engineering*, vol. 51, No. 6, pp. 1073-1076, 2004.

[10] A. Rakotomamonjy and V. Guigue, "BCI Competition III: Dataset II-Ensemble of SVMs for BCI P300 Speller," *IEEE Transactions on Biomedical Engineering*, vol. 55, No. 3, pp. 1147-1154, 2008.

[11] V. Vapnik, *Statistical learn ing theory* Springer, Berlin Heidelberg New York, 1998.

[12] J. C. Burges, "A tutorial on support vector machines for pattern recognition," *Data Mining and Knowledge Discovery* vol. 2, No. 2, pp. 121-167, 1998.

[13] A. L. Edsinger, "Robot manipulation in human environments," Doctor of Philosophy Doctoral Dissertation, Department of Electrical Engineering and Computer Science, Massachusetts Institute of Technology, Cambridge, 2007.

[14] A. De Luca, A. Albu-Schaffer, S. Haddadin, and G. Hirzinger, "Collision detection and safe reaction with the DLR-III Lightweight manipulator arm," *IEEE Int. Conf. on Intelligent Robots and Systems*, Beijing,Chinese, 2006, pp. 1623-1630.

[15] D. W. Robinson, "Design and analysis of series elasticity in closed-loop actuator force control," Doctor of Philosophy Doctoral Dissertation, Department of Mechanical Engineering, Massachusetts Institute of Technology, Cambridge, 2000.
[16] M. Thulasidas, G. Cuntai, and W. Jiankang, "Robust classification of EEG signal for brain-computer interface," *IEEE Transactions on Neural Systems and Rehabilitation Engineering*, vol. 14, No. 1, pp. 24-29, 2006.
[17] Y. H. Liu, H. P. Huang, and C. H. Weng, "Recognition of Electromyographic Signals Using Cascaded Kernel Learning Machine," *IEEE/ASME Transactions on Mechatronics*, vol. 12, No. 3, pp. 253-264, 2007.
[18] N. V. Thakor, "Biopotentials and Electrophysiology Measurement," *The Measurement. Instrumentation and Sensors Handbook*, Boca Raton,CRC Press, 1999.
[19] Y. H. Liu, "Feature analysis and classifier design and their applications to pattern recognition and data mining," *Department of Mechanical Engineering, National Taiwan University*, 2003.
[20] D. Zhang and G. Lu, "Generic Fourier descriptor for shape-based image retrieval," *IEEE International Conference on Multimedia and Expo*, Lausanne, Switzerland, 2002, pp. 425-428 vol.1.